Petroleum Science 20 (2023) 3830–3840

Contents lists available at ScienceDirect

Petroleum Science

journal homepage: www.keaipublishing.com/en/journals/petroleum-science

Original Paper

The influence of composition of asphaltenes of different genesis on the properties of carbon materials manufactured from them by plasma processing

Evgeniya Frantsina [a, b, *], Yuliya Petrova [a], Valentina Arkachenkova [a], Andrey Grin'ko [a], Alexander Pak [b], Pavel Povalyaev [a, b], Dmitry Zelentsov [a], Kirill Cherednichenko [c]

[a] Surgut State University, Institute of Natural and Technical Sciences, pr. Lenina 1, 628412, Surgut, Russian Federation
[b] Tomsk Polytechnic University, Laboratory of Advanced Materials for the Energy Industry, pr. Lenina, 30, 643050, Tomsk, Russian Federation
[c] National University of Oil and Gas Gubkin University, Department of Physical and Colloidal Chemistry, pr. Lenina, 65, 119991, Moscow, Russian Federation

ARTICLE INFO

Article history:
Received 31 October 2022
Received in revised form
23 March 2023
Accepted 12 July 2023
Available online 13 July 2023

Edited by Jia-Jia Fei

Keywords:
Asphaltenes
Natural asphaltite
Carbon materials
Nanomaterials
Plasma treatment
Graphite

ABSTRACT

The results of experimental studies of carbon materials, which are formed in the plasma of a direct current (DC) arc discharge initiated in open air from the asphaltenes of different origins, extracted from the natural asphaltite and from the oil of the Sredne-Ugutskoye Oilfield, are presented. The influence of the initial asphaltene composition on the composition and properties of the resulting carbon materials is analyzed. The initial asphaltenes and the samples of the carbon materials are characterized by the methods of X-ray diffraction, differential thermal analysis, X-ray fluorescence analysis, IR-Fourier spectroscopy, laser diffraction, transmission and scanning electron microscopy. The changes in the composition and structure of the asphaltenes are determined before and after their plasma treatment and the hypotheses are put forward concerning the chemical processes causing the changes in the molecular structure of the samples. As a result of plasma treatment of asphaltenes (100 A, 30 s), it was shown that graphitization occurs, as well as oxidation, and a decrease in sulfur content. Moreover, nanotubes and nano-onions have been detected using electron microscopy. Petroleum asphaltenes after plasma treatment give a less thermostable carbon material, but with a lower content of heteroatoms, and with a large amount of sulfur in the composition of sulfoxide structural fragments. This method is shown to be a promising technology for processing the petroleum feedstock enriched with heavy asphaltene components for the manufacture of carbon nanomaterials: nanotubes, nano-onions and polyhedral graphite.

1. Introduction

In view of depleting reserves of light oils, the extraction of highly viscous oils and natural bitumens with a content of asphaltenes and resins of up to 16–20 wt% and more has been rapidly growing in the recent time (Skibichkaya et al., 2016; Guo et al., 2016; Temizel et al., 2018). Asphaltenes are the high molecular heteroatomic substances and along with resins, they make up a significant part of heavy oils, bitumens, oil residues and wastes. The composition and content of asphaltenes can essentially vary depending on type of oils. Production, transportation and processing of these oils are labor-intensive due to, among other things, solidification of the asphaltenes at comparatively high temperatures and with pressure changes, which requires complex and costly technologies (Ganeeva et al., 2011; Ghabri et al., 2017, Abu-Khader and Speight, 2007). The molecular weight of asphaltenes is estimated at 500–2000 a.m.u. (Badre et al., 2006; Acevedo et al., 2005; Mullins et al., 2007), but it is difficult to determine the real value, since the asphaltene molecules have a high tendency to self-assembly and represent a polydisperse material. The studies of asphaltenes using X-ray and electron diffraction analyses demonstrated that they represent crystal-like structures with imperfect hexagonal close packing of carbon atoms (Galimova et al., 2015; Alhreez and Wen, 2019; Kananpanah et al., 2017). It is currently believed that there are two main structural types of asphaltene molecules, island (Mullins et al., 2007, 2010) and archipelago (Strausz et al., 2008; Chacon-Patino et al., 2018a, b). The structure

* Corresponding author. Surgut State University, Institute of Natural and Technical Sciences, pr. Lenina 1, 628412, Surgut, Russian Federation.
E-mail address: frantsinaev@gmail.com (E. Frantsina).

https://doi.org/10.1016/j.petsci.2023.07.012

and composition of asphaltenes may vary depending on the type of oil, depth of occurrence and time of genesis (Chacon-Patino et al., 2018; Cheshkova et al., 2019a, b; Zojaji et al., 2021; Mohammadi et al., 2021). With that, heavy oil asphaltenes (and asphaltenes from bitumens) most clearly differ from light oil asphaltenes, in particular, the difference lies in the molecular weights and metal content (Cheshkova et al., 2019b; Leyva et al., 2013; Gerasimova et al., 2022). Advances in AFM have made it possible to observe the structures of asphaltenes (Schuler et al., 2015, 2017). Moreover, it is possible to distinguish both island and archipelago structures. In addition, accurate fractionation of asphaltenes into many fractions of different nature and subsequent analysis of APPI-ICR-MS also made it possible to establish the presence of archipelago and island structures, and the predominance of a certain type of molecules depends on the nature of the sample (Chacon-Patino et al., 2017, 2018a, b).

Aside from to creating problems during extraction, processing and transportation of oil, asphaltenes may be of practical interest. Thus, kinetic studies of the thermal destruction of asphaltenes can be used to obtain critical information about the thermal maturity of oil, its history, and its likely migration routes (Di Primio et al., 2000). Soft thermolysis of asphaltenes and analysis of their degradation products, especially polycyclic biomarkers, are widely used in oil and gas prospecting geochemistry (Gordadze et al., 2015, 2018). There is also increasing attention to asphaltenes from the point of view of obtaining new carbon and composite materials from them (Kamkar and Natale, 2021; Han et al., 2019), in particular carbon fibers (Saad et al., 2022), and asphaltenes can be used as a component to improve the physicochemical characteristics of polymeric materials (Siddiqui et al., 2018; Kamkar and Natale, 2021).

For instance, graphene sheets were synthesized from asphaltenes in work (Xu et al., 2013) by calcination on vermiculite layers. Moreover, the authors managed to obtain a nitrogen-doped (N-doped) graphene-carbon nanotube (G-CNT) hybrid by preliminary adsorption of melamine on vermiculite. The resulting graphene materials were tested as anodes for lithium-ion batteries and demonstrated improved capacity and performance characteristics compared to the widely used reduced graphene oxide (rGO) (Xu et al., 2013). A similar method was used in (Wu et al., 2019) to obtain graphene sheets using montmorillonite as a substrate. The resulting materials (graphene sheets, graphene oxide, reduced graphene oxide) could be useful in a number of engineering and industrial applications, in particular, in microelectronics (Xu et al., 2013; Wu et al., 2019; Montanari et al., 2017; Jung and Bielawski, 2019). In work (AlHumaidan et al., 2022), a thermal method (carbonization) was used to obtain useful carbon materials. The result is achieved by eliminating alkyl side chains, exfoliating the aromatic layers and increasing the diameter of the aromatic sheet.

However, a few works are devoted to the study of plasma methods for the processing of asphaltenes, in particular, to the study of carbon materials obtained from them. Previously, work was carried out on the processing of asphaltenes in plasma in air medium (Villa et al., 2010) and in hydrogen (Poveda et al., 2014). In general, a structure similar to that of asphaltenes is retained, but oxygen-containing functional groups are added in the air medium.

Among the currently promising methods for synthesizing carbon materials (CMs) in an open air medium from asphaltenes is the plasma treatment in a DC arc discharge, which is a relatively simple and economically efficient process. It was successfully used in manufacturing carbon nanomaterials (Arora and Sharma, 2014; Letenko et al., 2010; Raznoushkin et al., 2015). This process relies on a self-supporting gas medium of carbon monoxide and dioxide (Pak et al., 2022), which rules out the necessity to use the vacuum and gas-generating equipment for creating a gas medium during the synthesis. In our previous work (Petrova et al., 2022) during the processing of petroleum asphaltenes in the plasma of an electric arc discharge at a current salt of 100 A (time 30 s) a new product was achieved – a graphite-like carbon material.

Thus, in our approach, we propose to use the technology of plasma treatment of asphaltenes in an arc discharge reactor, which will make it possible to obtain carbon materials at a relatively low cost. As well as in the present study, the influence of the feedstock on the properties of the resulting carbon material is determined. In this regard, it is also necessary to study the effect of the composition and properties of the initial asphaltenes on the carbon materials obtained from them.

The purpose of this work is to study the influence of the composition of asphaltenes of different genesis on the properties of carbon materials formed as a result of the plasma treatment in an DC electric arc reactor.

2. Materials and methods

2.1. Sample characterization and asphaltenes separation

The initial materials were the asphaltenes extracted from the oil of the Sredne-Ugutskoe Oilfield (SU oil, asphaltenes AS) and the natural asphaltite (asphaltenes AA). The oil of this deposit is characterized as sulfurous (1.33 wt%), low-viscosity (1.17 mPa•s), medium paraffin (2.92 wt%), light (density 783 kg/m^3) crude oil. Natural asphaltite (Ivanovskoye deposit, Orenburg region, density 1110–1220 kg/m^3) is characterized by a high content of sulfur (approx. 7.5 wt%) and asphaltenes (approx. 69 wt%) (Antipenko, 2013; Antipenko et al., 2020; Antipenko and Goncharov, 2011; Gordadze et al., 2018). The asphaltenes were extracted from the crude oil and natural asphaltite using standard SARA procedures (Fan et al., 2002; Cheshkova et al., 2019b). Briefly, 40:1 (*v*/*v*) *n*-hexane were added to the oil sample and the mixture was kept during the day. Then, the precipitated crude fraction of asphaltenes was purified from maltenes in a soxhlet apparatus with hexane for a day. The resulting asphaltenes were dried in vacuum to a constant weight, and stored in the dark to avoid photooxidation processes. In the present work, we compare the results of examination of CMs made from the asphaltenes extracted from oil (CMAS) and from the natural asphaltite (CMAA). The main stages of the process were as follows: 1. Precipitation and purification of asphaltenes. 2. Loading asphaltenes into an arc reactor for conducting a plasma treatment process. 3. Setting the operating mode of the reactor, conducting the process. 4. Collection of carbon material from the reactor. 5. Analysis of the obtained carbon materials and their comparison with the initial asphaltenes.

2.2. Plasma treatment of asphaltenes

A vacuum-free DC electric arc reactor with a horizontal electrode arrangement was used in the experiments for producing carbon materials from asphaltenes (Fig. 1) (Pak et al., 2022a, b). This configuration of the electrode arrangement ensures the formation of an arc discharge directly over the initial mixture, which allows plasma processing of both liquid and dielectric materials. The process of arc discharge initiation occurs between two cylindrical graphite electrodes (10 mm diameter, 100 mm long). Electrodes are installed coaxially in the current holders, which are connected to the outputs of a DC power source (rectifier-inverter welding transformer Colt Condor 200), with the possibility of adjusting the current value in the range from 20 to 200 A. Due to the fact that the reactor uses a direct current source, one of the electrodes is the anode and the other is the cathode. The processed material is placed at the bottom of a graphite crucible (height 30 mm, diameter

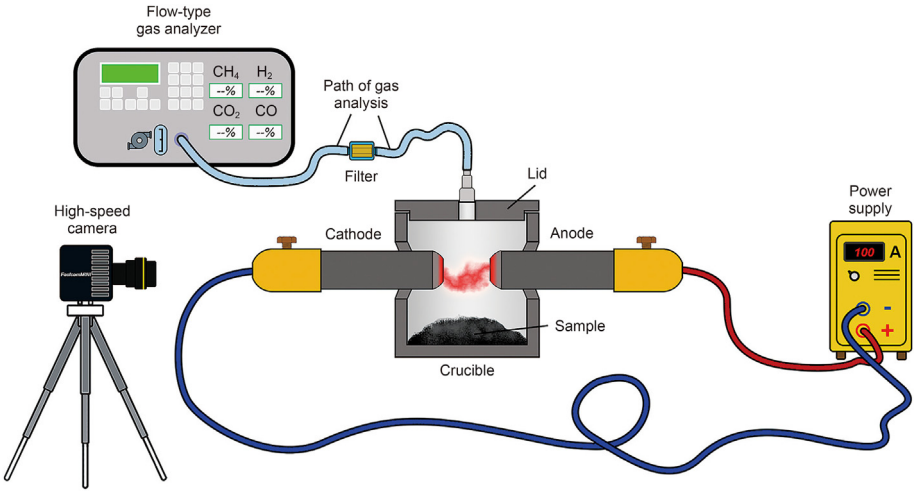

Fig. 1. Reactor for plasma processing of asphaltenes. Figure reprinted with author's permission (Petrova et al., 2022).

30 mm) with through holes for electrodes made coaxially. In this configuration, it is possible to load the initial mixture in an amount from 0.1 to 1 g and treatment duration of 120 s. In addition, the graphite crucible was closed from above with a graphite cover, where a through hole was made for installation of the gas path of the gas analyzer.

The current-carrying holder, where the anode is installed, is designed to be moved manually, so that after applying voltage to the electrodes, the anode is introduced into the graphite crucible, where the initial mixture is placed and the cathode is pre-positioned. When the anode and cathode come into contact, the system is short-circuited and after the anode is removed from the cathode, a discharge gap is formed, resulting in the ignition of an arc discharge. The moment of initiation and subsequent combustion of the electric arc discharge is accompanied by high temperatures (over 10,000 K at the place of arc discharge initiation (Zhao et al., 2013). After the material treatment process was completed, the arc was broken by retracting the anode to the start position. The resulting material was collected from the bottom of the crucible, and material was also formed on the surface of the graphite cap. The process of determining the operating modes of the asphaltene reactor is described in the previous work, the main criteria for selecting the mode are: the maximum hydrogen gas yield (4.11 mg) and the presence of a crystal structure in the resulting carbon. Thus, the mode for further research and treatment of asphaltenes was chosen (the burning time of the arc discharge was 30 s, the current set on the power supply was 100 A), also in the previous work the analysis of the gas medium was shown (Petrova et al., 2022). Subsequent experiments on asphaltene processing were performed in this mode. Also, in selecting the optimal operating mode, we took into account the minimum energy required for a complete processing of the initial mixture (power near 2.9 kW, released energy near 123 kJ). Table 1 shows the mass balance of the experiments performed.

2.3. Structural group analysis

The structural group analysis (SGA) was carried out as in the works (Cheshkova et al., 2019; Golovko et al., 2010, 2012). Briefly, it is based on the measurement of molecular weights, elemental composition and ^{1}H NMR spectroscopy of asphaltene samples. The elemental analysis of the samples was performed using a Vario EL Cube CHNS analyzer. The absolute error of the analyzer did not exceed ±0.1% for each analyzed element. The oxygen content was evaluated by the difference between 100% and the sum of C, H, N, and S elements. The molecular masses were measured by cryoscopy in naphthalene. ^{1}H NMR spectra were recorded using a Bruker Avance AV 300 NMR-Fourier spectrometer at 300 MHz in $CdCl_3$ solutions. A more detailed description is given in the supplementary materials.

2.4. X-ray diffraction method

Crystalline phases were identified by X-ray diffractometry on a Shimadzu XRD 7000s X-ray diffractometer (Shimadzu XRD 7000s, λ=1.5406 Å, step 0.02 deg, exposure 1 s per point, X-ray tube voltage 40 kV, current 30 mA). The qualitative analysis was carried out using the international structural database PDF4+.

2.5. TGA/DTA and DSC

Thermogravimetry (TGA) and differential scanning calorimetry (DSC) were carried out by differential thermal analysis (Mettler Toledo TGA/DSC 3+ Star System, heating rate 10 °C/min in the temperature range within 30–1050 °C) in an inert medium (nitrogen).

2.6. X-ray fluorescence analysis

The elemental composition of asphaltenes and carbon materials

Table 1
Conditions of the plasma treatment process and the yield of carbon materials.

Sample	Current, A	Time, s	Sample mass, g	Solid-phase yield from the sample mass, %	Change in crucible mass, g	Change in anode mass, g	Change in cathode mass, g	Change in the mass of the cover, g
AA/CMAA	100	30	0.4	62.62	0.2748	0.2123	0.965	0.0111
AS/CMAS			0.4	39.07	0.1353	0.1391	0.581	0.0556

was studied using an EDX-8000 (Shimadzu) X-ray fluorescence spectrometer. For that, EDX-8000 spectrometer operated at 15–50 kV (vacuum) for light (Na, Mg, K) and other elements (V, Cr, Fe, Rb, Cs) with software quantitative analysis (fundamental parameter method).

2.7. FTIR

Samples for FTIR were prepared as potassium bromide (KBr) pellets, containing 0.6 wt% of powdered samples. Potassium bromide (KBr) was grounded in agate mortar and kept in an oven at 650 °C for 6–8 h in order to remove water and other potential impurities. Mixtures of sample/KBr were prepared in a clean and dry agate mortar. The pellets were dried under a vacuum before the experiment. The analysis was performed on a PerkinElmer Spectrum 100 spectrometer (transmission mode, 700–4000 cm^{-1}). During acquisition, 25 scans per sample were collected at a resolution of 4 cm^{-1}.

2.8. Laser diffraction method

Suspension of the resulting CMs in 0.12% sodium oleate was filled in a cuvette, and particle size was recorded in five successive trials using a laser light diffraction particle size analyzer (SALD-2300, Shimadzu Corporation) with software SHIMADZU WingSALD II version 3.1.0. The mean, median, and modal of different particles (%) with varying sizes were then noted.

2.9. Electron microscopy

Initial asphaltenes and the resulting CMs also were characterized using the methods of transmission (JEOL JEM 2100F) and scanning electron microscopy (Tescan Vega 3 SBU with an Oxford Instruments X-Max-50 EDS detector, JEOL JSM-6460LV).

3. Results and discussion

The conditions and the mass balance of the plasma processing of asphaltenes are shown in Table 1. As a result of plasma treatment of asphaltenes, a different yield of carbon materials (solid phase) was observed, which, apparently, depends on the nature of the raw material used, its composition, structural characteristics and thermal stability. According to the results of the differential thermal analysis (Fig. 2), crude oil asphaltenes (AS) are less stable thermally than those extracted from asphaltite (AA) and, hence, the solid-phase yield after their plasma processing is smaller.

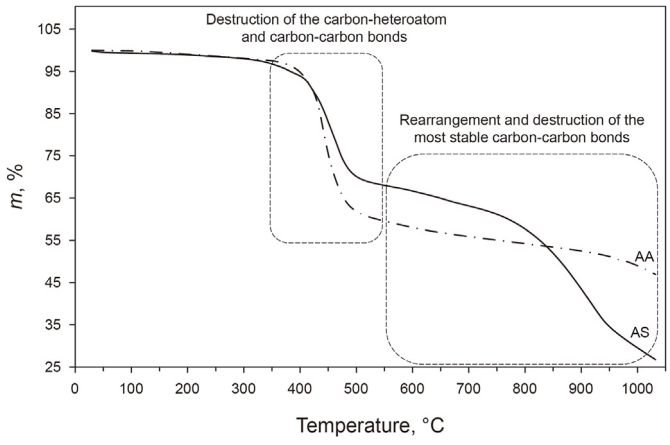

Fig. 2. TGA curve of asphaltene samples from oil (AS) and asphaltite (AA) in the inert atmosphere (N_2).

3.1. Thermogravimetric analysis

The results of a thermogravimetric analysis (TGA) of the initial asphaltene samples (Table 2, Figs. 2 and 3) and the carbon materials produced from them (Table 3, Fig. 5) are presented as the thermogravimetry and differential (DTA) curves characterizing the temperature profiles of their decomposition in the inert medium.

A fast-thermal decomposition of the AA sample starts at 350 °C and ends at 550 °C, accompanied by the maximum weight loss rate at 454 °C (Figs. 2 and 3, Table 2). At 550 °C, the thermal decomposition rate decreases, but the destruction continues up to 1030 °C (Kopytov and Golovko, 2017). At the temperatures higher than 1030 °C, the residue is conventionally determined as coke. The weight loss at 350–550 °C is found to be 37.97 wt%, and in the interval of 550–1030 °C was 12.78 wt%. The total weight loss of the AA asphaltenes is 53.12 wt%. The steepness of the TGA curve (AA) suggests a narrow molecular-mass distribution (Douda et al., 2004).

A decomposition of the AS asphaltenes starts at 350 °C and first phase of intensive destruction ends at 550 °C, with the maximum weight loss occurring at 464 °C (Figs. 2 and 3, Table 2). This temperature interval corresponds to an intensive destruction of the carbon-heteroatom (up to 410 °C) and carbon-carbon (410–550 °C) bonds in the naphthenic-aromatic core of the molecules still retaining their stability despite the intermolecular rearrangements accompanied by the splitting of hydrogen and the formation of graphite-like structures (Grinko and Golovko, 2014; Dolomatov et al., 2020; Kopytov and Golovko, 2017). At 760 °C, the weight loss rate of this sample keeps increasing up to the temperature of 970 °C, forming a second peak on the DTA curve at 930 °C (Fig. 3), which suggests a molecular rearrangement and destruction of the most stable carbon-carbon bonds in the cores of the asphaltenes molecules (Grinko and Golovko, 2014; Dolomatov et al., 2020). Further on, the extraction of volatile components becomes slower but still continues up to 1030 °C. The total weight loss of the sample was found to be 73.26 wt%. Note that the weight loss in the temperature interval within 350–550 °C was 29.05 wt% and within 750–1030 °C was 34.75 wt%, respectively. The presence of the second peak at 930 °C in the TGA curve of AS asphaltenes may indicate a greater number of less stable carbon-carbon bonds in the naphthenic-aromatic cores of asphaltene molecules compared to those from the natural asphaltite sample (AA).

An endothermic effect is observed on the differential scanning calorimetry (DSC) curves of the asphaltene samples (Fig. 4, Curves A and AS) at the temperatures higher than 400 °C, which corresponds to an intensive destruction characteristic of the X-ray amorphous phase. On the DSC curves of the asphaltenes from the SU oil (Fig. 4, Curve AS) there is an intensive endothermic process in the region of 750–1030 °C with a maximum at 930 °C, which is associated with a characteristic feature of their structure, apparently the presence of a larger amount of less thermally stable bonds in the naphthenic-aromatic framework of asphaltene molecules. Note a much higher rate of thermal decomposition of the AS sample compared to that of the (AA) sample, which is due to a larger number of the labile C–C

Table 2
Thermal analysis results of asphaltene samples from oil (AS) and asphaltite (AA).

Temperature ranges, °C	Weight loss, wt%	
	AA	AS
30–350	2.37	2.88
350–550	**37.97**	**29.05**
550–750	4.50	6.58
750–1030	8.28	**34.75**
30–1030	**53.12**	73.26

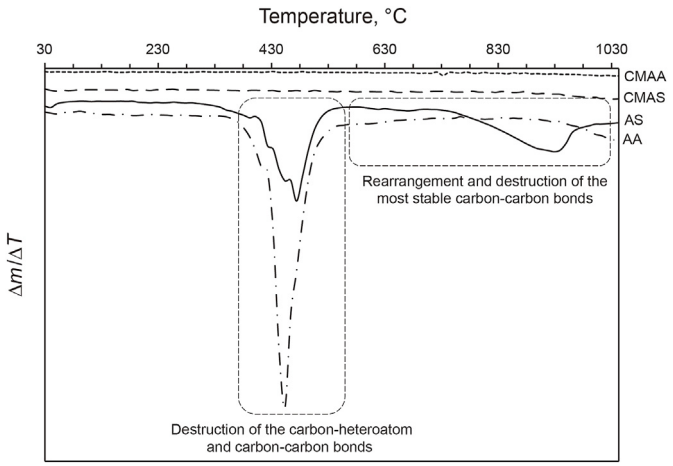

Fig. 3. DTA curves of the samples in the inert atmosphere (N_2): CMAA, a carbon material derived from asphaltenes of asphaltite; CMAS, a carbon material derived from asphaltenes of SU oil; AA, asphaltenes of asphaltite; AS, asphaltenes of SU oil.

Table 3
Differential thermal analysis of the resulting carbon materials.

Temperature interval, °C	Weight loss, wt%	
	CMAA	CMAS
30–820	0.54	2.72
820–1030	0.92	4.03
Total	1.46	6.75

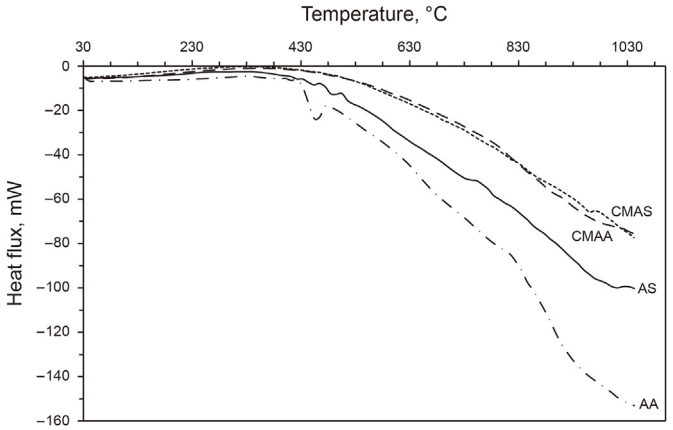

Fig. 4. DSC analysis of the carbon materials in the inert (N_2) atmosphere: CMAA, a carbon material derived from asphaltenes of asphaltite; CMAS, a carbon material derived from asphaltenes of SU oil; AA: asphaltenes of asphaltite; AS, asphaltenes of SU oil.

and C–heteroatom bonds in the molecular structure of the AS asphaltenes.

The TGA curves (Fig. 5) for the carbon materials (CMAA and CMAS) manufactured by the plasma processing of asphaltenes do not have any pronounced weight loss peaks. For both samples, the weight loss occurs within the interval of 30–1030 °C, with more than a half of the total weight loss of the samples falling within the high-temperature region of 820–1030 °C. The difference consists in the fact that the CMAS sample exhibits a large total weight loss (6.75 wt%), while the CMAA sample is 1.46 wt% (Table 3). This is due to the prevailing content of graphite-like structures in the composition of CMAA.

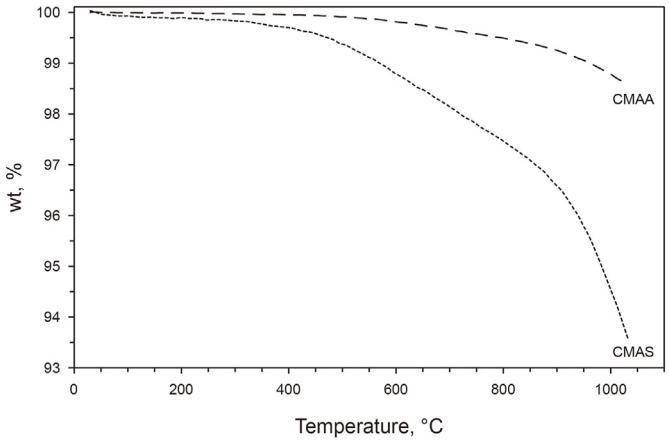

Fig. 5. TGA curves of carbon material formed in the inert (N_2) environment: CMAA, a carbon material derived from asphaltenes of asphaltite; CMAS, a carbon material derived from asphaltenes of SU oil; AA: asphaltenes of asphaltite; AS, asphaltenes of SU oil.

3.2. X-ray diffraction analysis

The phase analysis of the carbon materials (CMAS and CMAA) was performed by the method of X-ray diffraction (XRD). The reflections of a graphite-like structure were indexed on the XRD patterns (Fig. 6).

The XRD and DTA data demonstrated that carbon materials of amorphous and graphite like structures are formed as a result of processing of the asphaltenes in the DC arc-discharge plasma. One can clearly see the difference between the obtained carbon materials and the initial asphaltenes (Figs. S2, S3 and 6). As a result of the plasma processing of asphaltenes, structuring (graphitization) increases, and the degree of crystallinity increases (from ~25% in the initial asphaltenes to ~45% in corresponding carbon materials). At the same time, as a result of plasma treatment, different asphaltenes give different carbon materials, the content of the amorphous phase in which is also different, which affects their thermal stability (Fig. 5, Table 3). For comparison, we have shown the graphite XRD data (see Fig. S1) and initial asphaltene samples (Figs. S2 and S3). As can be seen, the structure of the graphite sample is similar to the structure of the obtained carbon materials. At the same time, the X-ray diffraction patterns of the initial asphaltenes are very different from those of carbon materials; asphaltenes are less structured and contain more amorphous phase (Petrova et al., 2022).

3.3. Energy dispersive X-ray fluorescence analysis

Using the method of energy-dispersive X-ray fluorescence analysis (EDXF), a large number of elements were determined in the compositions of the initial asphaltene samples and the manufactured carbon materials (Table 4).

The fraction of carbon in the AS asphaltenes is smaller but the content of all determined elements except carbon is larger (91.2 and 8.8 wt%, respectively) compared to the AA asphaltenes (98.1 and 2.0 wt%, respectively). This is explained by the conditions of formation in the reservoir and presumably by the fact that oil is more in contact with reservoir waters (Kayukova et al., 2015; Gordadze et al., 2018). It is likely that AA asphaltenes contain less labile C–S and C–O bonds, since their degradation onset temperature is higher (350 °C, Fig. 2) compared to AS asphaltenes (310 °C) (Grinko and Golovko, 2014). This fact may also be associated with a lower content of other elements in AA asphaltenes (Table 2). The AS asphaltenes are enriched in Ca, Mg, Na, Cl, K, Si, which is likely to be

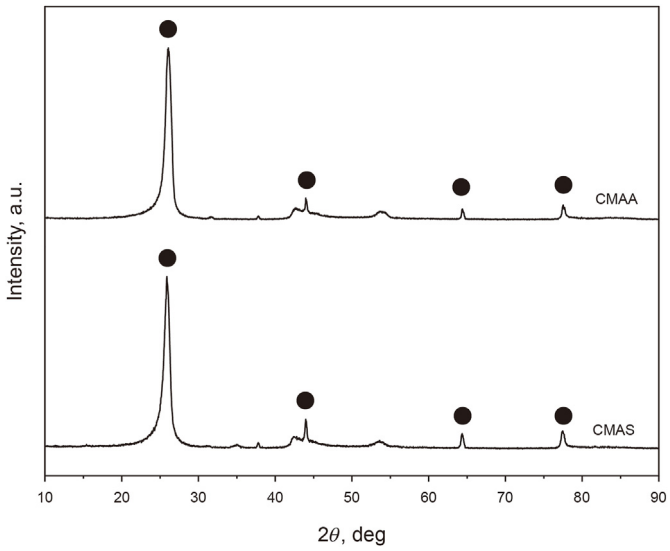

Fig. 6. XRD patterns from the manufactured carbon materials (graphite-like structure denoted by symbol ●): CMAA, a carbon material derived from asphaltenes of asphaltite; CMAS, a carbon material derived from asphaltenes of SU oil.

Table 4
EDXF analysis results of the initial asphaltene samples (AS and AA) and the manufactured carbon materials from them (CMAS and CMAA).

Element	Elemental composition, wt%			
	Initial asphaltenes		Carbon materials	
	AS	AA	CMAS	CMAA
C	91.2	98.1	99.7	98.8
S	0.5	1.8	0.1	1.0
Na	6.920	<0.010	<0.010	<0.010
Cl	1.065	0.023	0.043	<0.001
Ca	0.084	0.007	0.017	0.019
Mg	0.050	<0.010	<0.010	<0.010
Si	0.037	0.022	0.041	0.017
Al	<0.001	0.022	0.022	0.013
Fe	0.002	0.002	0.010	0.015
V	<0.001	0.038	0.006	0.113
Ni	<0.001	0.004	<0.001	0.010
K	0.004	0.001	0.001	0.002

due to a stronger impact of the stratal water and peculiarities of the oil-enclosing reservoir rock composition (Meshurova and Khodyashev, 2018). The AA sample of the natural asphaltite has a large content of V, Ni, and Fe, which are part of the composition of the porphyrinic structural fragments, which could be attributed to the characteristic features of the asphaltite deposition facies conditions (Krayushkin et al., 2008).

It should be noted that the contents of V, Ni and Fe increases in carbon material compared to the initial asphaltenes due to their concentration in the carbon residue after the considerable destruction and rearrangement of the naphthenic-aromatic core of the asphaltene molecules (Poveda et al., 2014; Villa et al., 2010).

As a result of plasma processing, the content of carbon in both asphaltene samples increases from 91.2 to 99.7 wt% (AS) and from 98.1 to 98.8 wt% (AA). Note that the content of sulfur decreases from 0.5 to 0.1 wt% (for AS) and from 1.8 to 1.0 wt% (for AA). This tendency is observed because of the destruction processes and breaking of the less stable carbon-sulfur bonds, in particular, those in the sulfide structural fragments of the asphaltenes molecules (Grinko and Golovko, 2014; Golovko and Grinko, 2018).

The content of the other elements on the whole tends to decrease, with some fluctuations observed (an increase of Si and Al upon processing of the AS sample and an increase of Ca in the case of AA sample), which could be due to the peculiarities of a non-homogeneous distribution of these elements in the asphaltenes molecule structure; furthermore, these elements are in the occluded state and under plasma processing are concentrated in the solid residue.

The analyses of the composition and structure of the asphaltenes and the carbon materials manufactured from them via plasma processing suggest a conclusion that there occurs a process of graphite structure formation, accompanied by a change in the elemental composition towards an increase in the carbon content, a decrease in the sulfur content and an increase in the fraction of such heavy elements as V, Ni, and Fe.

3.4. SGA and FT-IR spectroscopy

The FT-IR spectroscopic examination of the CM samples revealed the processes of an oxidative destruction of the forming graphite-like structures. The FT-IR spectra of the resulting carbon materials (Fig. 7) contain the vibrational bands of the hydroxyl group in the region of 3300–3600 cm^{-1}, where a shoulder near ~3300 cm^{-1} corresponds to the stretching vibrations of a hydroxyl group of the graphite oxide (Hontoria-Lucas et al., 1995). In the CMAS sample, these bands are more pronounced compared to those in CMAA, which also supports the influence of the composition of the initial petroleum asphaltenes with a large number of C–C and C–heteroatom bonds tending to oxidation compared to the asphaltenes of the natural asphaltite.

Although, according to the XRD data, the structure of the synthesized carbon materials is close to the structure of graphite, however, according to FTIR spectrometry data, we can see that they are quite different in chemical composition (Katrick et al., 2013; Ţucureanu et al., 2016) (see IR spectrum of graphite Fig. S3), since carbon materials in their composition have quite a lot of different functional groups, which could also be formed due to secondary processes during plasma treatment.

Structural group analysis showed that AA asphaltenes differ

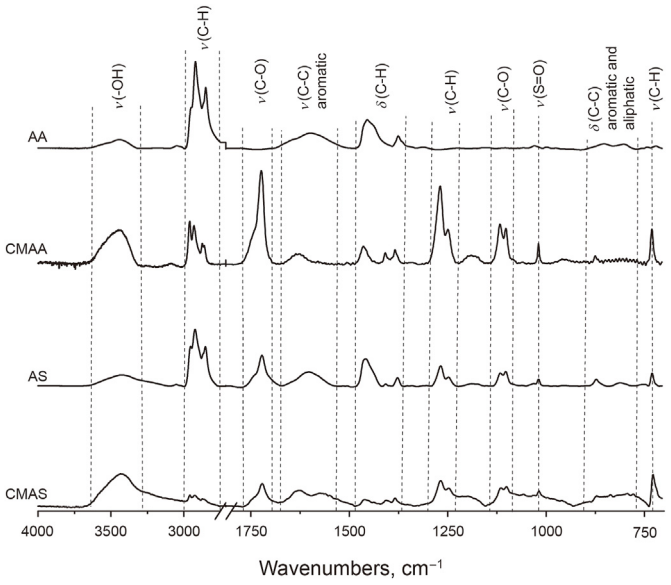

Fig. 7. FTIR spectroscopy of the samples: CMAA, a carbon material derived from asphaltenes of asphaltite; CMAS, a carbon material derived from asphaltenes of SU oil; AA, asphaltenes of asphaltite; AS, asphaltenes of SU oil (absorbance for AA and AS samples is 0.01–0.34 and for CMAA and CMAS samples is 0.001–0.06).

from AS asphaltenes. Asphaltenes AA has a high degree of aromaticity and contains more carbon atoms in the paraffin chains (Table S3).

The vibrational bands at 1720 cm^{-1} and 1080–1140 cm^{-1} belong to the hydroxyl stretching vibrations on the edges of the flat graphite structures and the conjugated carbonyl vibrations (Asemani and Rabbani, 2015; Socrates, 2004), which also proves the oxidation of the forming graphite-like structures.

The band in the region of 1580–1650 cm^{-1} of the asphaltene samples (Fig. 7, AS, AA) belong to the C–C stretching vibrations in the conjugated aromatic systems (structural blocks of asphaltenes) (Asemani and Rabbani, 2015), and in the case of carbon materials (Fig. 7, CMAS, CMAA) these bands can be attributed to the C–C bonds in graphene sheets (Tikhomirov and Kimstach, 2011; Tucureanu et al., 2016), which validates the process of asphaltene graphitization.

The band near 1030 cm^{-1} corresponds to the vibrations of the S=O groups, whose content can both decrease or increase (depending on the position of the functional group in the asphaltene molecules) (Asemani and Rabbani, 2015; Villa et al., 2010).

Based on the FT-IR spectra, we calculated the integral spectral coefficients, which allowed performing a semi-quantitative comparative analysis of the initial asphaltene samples and the resulting carbon materials (Table 5) (Grinko and Golovko, 2011; Glebovskaya, 1971; Ivanova et al., 2008). The normalization during the calculation of these coefficients is commonly performed with respect to the intensity of the C–H band vibrations in the methylene groups of the aliphatic structural fragments (1460 cm^{-1}) (Grinko and Golovko, 2011; Glebovskaya, 1971). In the present work, the following coefficients were applied (Villa et al., 2010; Grinko and Golovko, 2011; Glebovskaya, 1971; Ivanova et al., 2008): aromaticity index Ar = I_{1597}/I_{1460}; degree of branching of paraffin fragments Bn = I_{1375}/I_{1460}; oxidation level Ox = I_{1710}/I_{1460}; relative content of sulfoxide moieties SO = I_{1030}/I_{1460}.

Asphaltenes AA have a slightly higher degree of aromaticity, more branching of paraffin chains and a lower degree of oxidation compared to sample AS. This conclusion is consistent with the SGA data: parameter f_a for asphaltenes AA is higher (see Table S3). The branching of paraffin structures in AA asphaltenes is higher, which also agrees with the SGA data.

Under the conditions of plasma processing, we observed a decrease of the degree of aromaticity of the AA sample, a smaller branching of the paraffin chains, and a reduced content of the sulfoxide structural moieties SO, while an opposite tendency is observed for the AS sample. An increase in the proportion of carbonyl and carboxyl groups also confirms an increase in the degree of oxidation of the samples of carbon materials (Fig. 7).

A lower aromaticity index of the (AA) sample subjected to plasma processing could be due to its transformation to the carbon modification, e.g., graphite-like structures not possessing classical aromaticity and, hence, not increasing the vibrational band near ~1600 cm^{-1}, while it is very likely that aromatic structures are formed following the plasma treatment of the (AS) sample.

Table 5
Spectral coefficients of the initial asphaltene samples and the resulting carbon materials calculated from IR spectra.

Sample	Coefficients			
	Ar	Bn	Ox	SO
AA	0.589	0.470	0.001	0.090
CMAA	0.115	0.313	1.128	0.001
AS	0.503	0.265	0.489	0.082
CMAS	1.576	0.644	1.775	1.627

An increased content of the sulfoxide moieties (SO coefficient) during the plasma treatment of the (AS) sample is likely to be due to the oxidation of sulfur found in the sulfide structural fragments, including those entering the paraffin chains, whose number in the AS structure is larger than in AA (Table 4). This could be related to their lower thermal stability that of the AA asphaltenes.

Generally, the results obtained in this study support the oxidative destruction of asphaltenes in the arc-discharge plasma, resulting in the formation of graphite-like structures due to the secondary radical reactions and rearrangement reactions. Their kinetics and thermodynamics determine the ratio between the graphite-like, aromatic, oxidized and other fragments in the resulting carbon materials, whose composition would depend on the initial feedstock.

3.5. Laser diffraction

The results obtained by the method of laser diffraction demonstrated that the particle size distribution (q, %) of the asphaltene samples has a polymodal pattern; the particle sizes (D, μm) lie within the range from 0.5 to 300.0 μm, the average particle diameter being 18.8 μm (Fig. 8).

The average size of the particles of the AS samples after their processing in the arc-discharge plasma decreases to 2.0 μm (Table 6), and a wider fraction contains the particles with the sizes from 0.1 to 10.0 μm (Fig. 8, CMAS). For the AA samples, the average particle size increases to 16.9 μm (Petrova et al., 2022). These particle size changes could be due to both the increased carbon content and the degree of graphitization in the carbon materials and, more so, to the structural features of the initial asphaltenes, as well as some surface phenomena requiring further research (Dolomatov et al., 2020).

3.6. Electron microscopy

The sample manufactured by the plasma treatment of asphaltenes extracted from the oil of the Sredne-Ugutskoye Oilfield (CMAS) was examined using the methods of transmission (Fig. 9) and scanning electron microscopy (Fig. 10). It is seen in the panoramic image (Fig. 9(a)) that the synthesized product contains such crystalline graphite-like nanostructures as: 1. polyhedral graphite (PG) (Song et al., 2007), 2. graphite nanotubes (Su et al., 2014) and 3. nano-onions (Zhai et al., 2020).

The presence of different morphological types of nanostructures in the product might have been caused by the feedstock

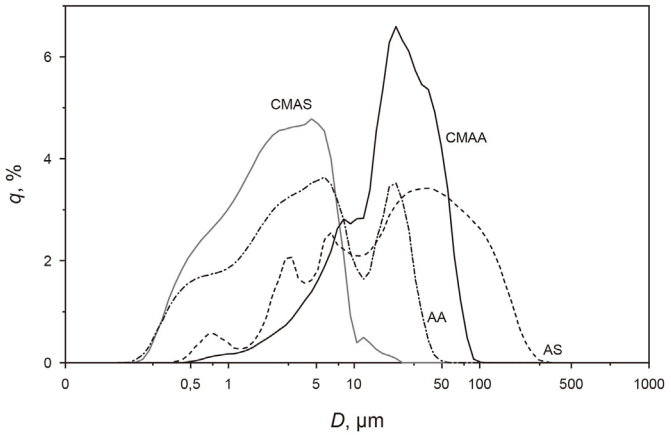

Fig. 8. Particle size distribution in the samples of asphaltenes (AA and AS) and carbon materials (CMAA and CMAS).

Table 6
Particle size distribution in the asphaltene samples and in corresponded CMs.

Name	Average particle diameter, μm	Median, μm	Mode, μm
AA	3.7	3.9	5.8
CMAA	16.9	19.7	19.0
AS	18.8	22.8	38.8
CMAS	2.0	2.2	4.6

inhomogeneity, since asphaltenes can contain a large number of impurities, which is demonstrated by the EDS analysis. The design peculiarities of the discharge circuit exert a direct influence on the formation of graphite-like structures due to the features of the temperature field distribution and the operation principles of electric-arc reactors (Gomez et al., 2009).

The sizes of polyhedral graphite particles in the synthesized product range from 150 to 260 nm (Usta et al., 2006). Fig. 9(b) presents a typical electron diffraction pattern for this type of particles, specifically, polycrystalline graphite particles. The size of nano-onions varies 26–150 nm, with the particles from 50 to 100 nm predominating.

The interplane distances (Fig. 9(b)) are consistent with those of the graphite-like structure within the acceptable error threshold. Due to the peculiar features of the synthesis, as mentioned above, the particle shapes are subject to deformations (Dhand et al., 2021), and the interplane distances can differ from their reference values, which is frequently reported by other authors (He et al., 2009; Bagautdinov et al., 2022).

According to the SEM studies (Fig. 10), the particles of the synthesized material are agglomerated; in this case the particle sizes are in the range from ~50 to ~400 μm. Under higher magnification, one can see that the structure of the agglomerates is porous and inhomogeneous.

A comparison of the images of carbon materials manufactured form the asphaltenes of the Sredne-Ugutskoye Oilfield with those of the natural asphaltite (Petrova et al., 2022) demonstrated that in both cases graphite-like structures of three types predominate in them, specifically: polyhedral graphite, nano-onions and nanotubes. The difference consists in the size of the carbon material agglomerates. The nature of this phenomenon is so far unclear; furthermore, the electric-arc processes are characterized by synthesizing products with a wide particle size distribution due to a high temperature gradient in the reaction zone.

4. Conclusions

1. A possibility in principle has been shown of forming graphite-like carbon materials from asphaltenes of different origin in the DC arc-discharge plasma ignited in an open air environment. The method is thought to be a promising process for conversion of the petroleum feedstock enriched in heavy asphaltene components (oil processing and petrochemical residues and wastes) yielding useful carbon materials for different fields of science and technology, which makes further research along this avenue very promising.

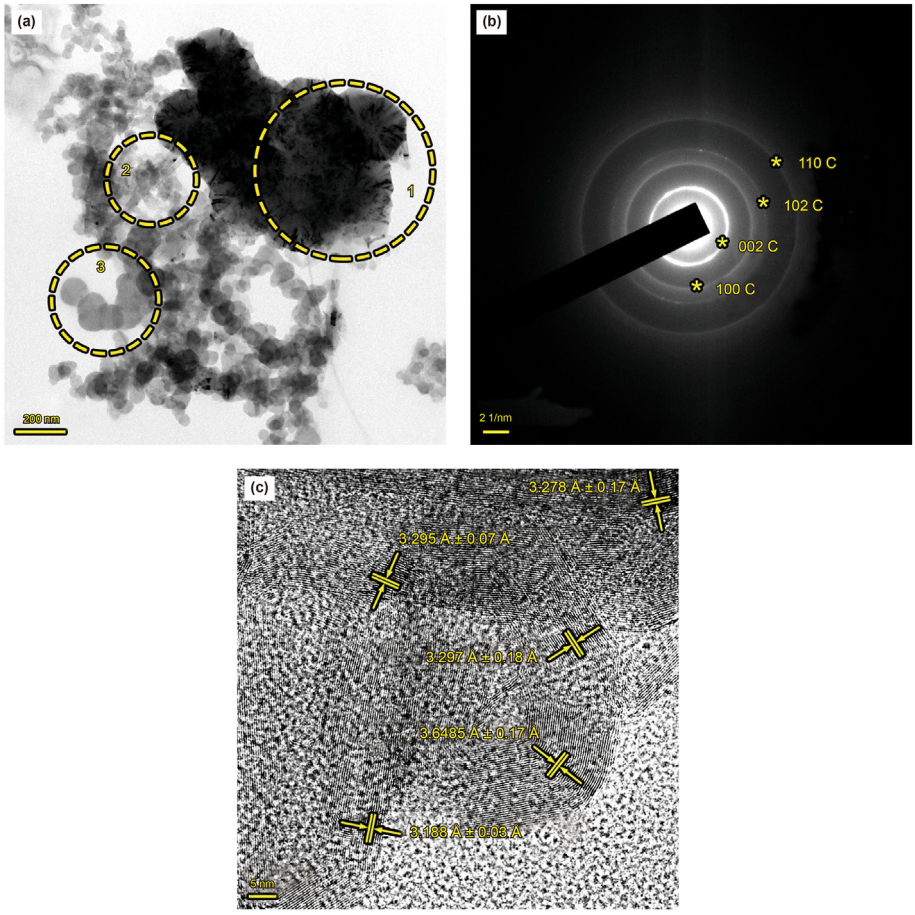

Fig. 9. TEM results of CMAS samples: (**a**) panoramic image of the synthesized product, (**b**) typical electron diffraction pattern, (**c**) direct-resolution image of the particles with indicated interplanar distances.

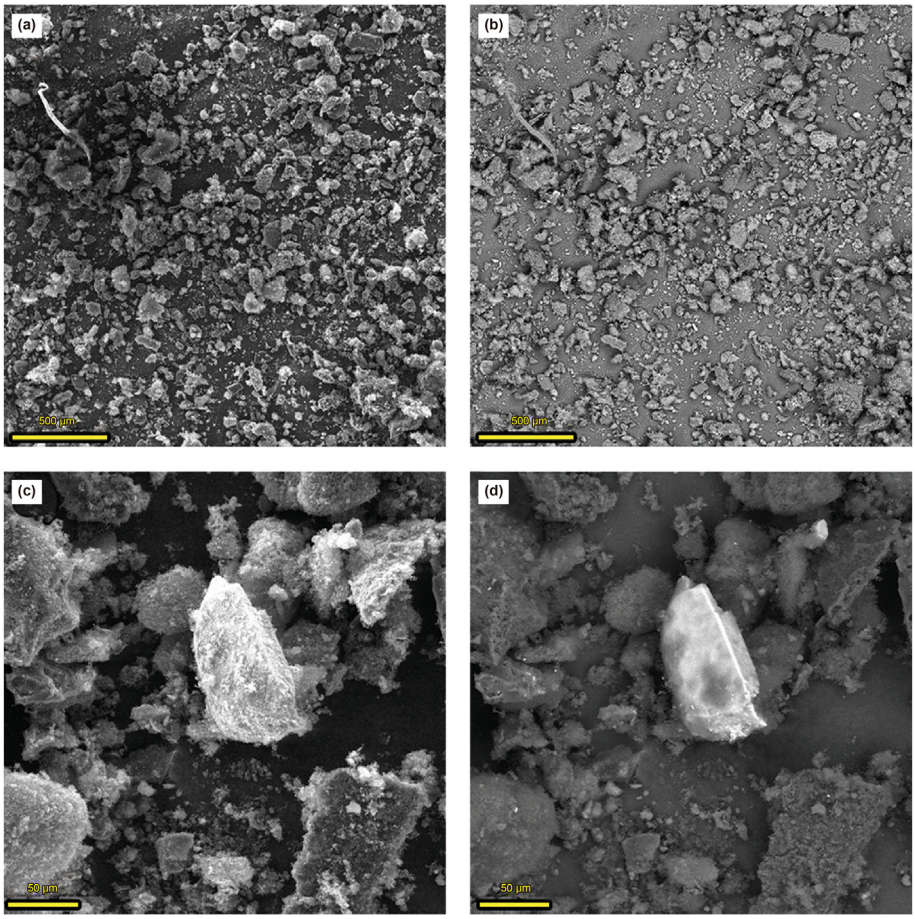

Fig. 10. SEM results of the synthesized product CMAS: (**a**) panoramic SE-image, (**b**) panoramic BSE-image, (**c**) SE-image at higher magnification, (**d**) BSE-image at higher.

2. The processing of asphaltenes in the DC arc-discharge plasma at the current of 100 A for 30 s causes an oxidative destruction of the asphaltene molecules along the weakest C–C and C–heteroatom bonds, accompanied by a simultaneous formation of graphite-like structures of various morphological types: polyhedral graphite, nanotubes and nano-onions. These types of structures predominate in asphaltenes of both origins. The differences are only in the size of the agglomerates of the obtained carbon nanomaterials. The elemental composition of the asphaltenes changes with a tendency towards a large fraction of carbon (from 91.2% to 99.7% for AS→ CMAS and from 98.1% to 98.8% for AA → CMAA), a reduced sulfur content (reduced ~69.2% for AS, and reduced ~45.1% for AA), and an increased concentration of such metals as vanadium, nickel, and iron (V and Fe increase by 60 and 5 times upon treatment of the AS sample, respectively; and V, Fe, and Ni increase by 3, 7.5, and 2.5 times upon treatment of the AA sample, respectively).
3. The petroleum asphaltenes (AS) are less thermally stable than those of the natural asphaltite (AA), which is due to peculiarities of their genesis in the reservoir. The petroleum asphaltenes contain a larger number of the weak C–C and C–heteroatom bonds tending towards oxidation, whose destruction starts at lower temperatures. Consequently, due to the structural features and composition of the initial petroleum asphaltenes the resulting carbon materials are less stable, which is validated by the data of thermal analyses and IR spectroscopy.
4. The plasma treatment causes the changes in aromaticity, oxidation level, paraffin chain branching, the content of sulfoxide structural fragments, sulfur content, and particle size, which is most likely related to the radical and rearrangement reactions resulting in the change of the material structure. It is the kinetics and thermodynamics of these reactions which determine the ratio of the resulting graphite-like, aromatic, oxidized and other fragments in the forming carbon materials, which shows a good promise for further research.

Declaration of competing interest

The authors declare that they have no known competing financial interests or personal relationships that could have appeared to influence the work reported in this paper.

Acknowledgments

This study was funded by a grant from the Russian Science Foundation (Project No. 22-13-20016) and carried out at the Surgut State University and Tomsk Polytechnic University.

Appendix A. Supplementary data

Supplementary data to this article can be found online at https://doi.org/10.1016/j.petsci.2023.07.012.

References

Abu-Khader, M.M., Speight, J.G., 2007. Influence of high asphaltene feedstocks on processing. Oil Gas Sci. Technol. 62 (5), 715–722. https://doi.org/10.2516/ogst:

2007049.
Acevedo, S., Gutierrez, L.B., Negrin, G., et al., 2005. Molecular weight of petroleum asphaltenes: a comparison between mass spectrometry and vapor pressure osmometry. Energy Fuel. 19, 1548–1560. https://doi.org/10.1021/ef040071.
Alhreez, M., Wen, B., 2019. Molecular structure characterization of asphaltene in the presence of inhibitors with nanoemulsions. RSC Adv. 9, 19560–19570. https://doi.org/10.1039/C9RA02664A.
AlHumaidan, F.S., Rana, M.S., Vinoba, M., et al., 2022. Synthesizing few-layer carbon materials from asphaltene by thermal treatment. Diam. Relat. Mater. 129, 109316. https://doi.org/10.1016/j.diamond.2022.109316.
Antipenko, V.R., Goncharov, I.V., 2011. Composition of the lube oil fraction of asphaltite from the Ivanovskoe field of Orenburg oblast. Petrol. Chem. 51, 330–336. https://doi.org/10.1134/S0965544111050033.
Antipenko, V.R., 2013. Thermal Transformations of High-Sulfur Natural Asphaltite: Geochemical and Technological Aspects. Nauka Press, Novosibirsk, Russia, p. 184 (in Russian).
Antipenko, V.R., Fedyaeva, O.N., Grinko, A.A., 2020. Structural parameters of resins and asphaltenes of natural asphaltite and products of its conversion in supercritical water. AIP Conf. Proc. 2310, 020022. https://doi.org/10.1063/5.0034692.
Arora, N., Sharma, N.N., 2014. Arc discharge synthesis of carbon nanotubes: comprehensive review. Diam. Relat. Mater. 50, 135–150. https://doi.org/10.1016/j.diamond.2014.10.001.
Asemani, M., Rabbani, A., 2015. Oil-oil correlation by FTIR spectroscopy of asphaltene samples. Geosci. J. 1–12. https://doi.org/10.1007/s12303-015-0042-1.
Badre, S., Goncalves, C.C., Norinaga, K., et al., 2006. Molecular size and weight of asphaltene and asphaltene solubility fractions from coals, crude oils and bitumen. Fuel 85, 1–11. https://doi.org/10.1016/j.fuel.2005.05.021.
Bagautdinov, B., Ohara, K., Babaev, A.A., 2022. High-energy X-Ray diffraction study of multiwalled carbon nanotubes fabricated by arc discharge plasma process. Carbon 191, 75–83. https://doi.org/10.1016/j.carbon.2022.01.038.
Chacon-Patino, M.L., Rowland, S.M., Rodgers, R.P., 2017. Advances in asphaltene petroleomics. part 1: asphaltenes are composed of abundant island and archipelago structural motifs. Energy Fuel. 31, 13509–13518. https://doi.org/10.1021/acs.energyfuels.7b02873.
Chacon-Patino, M.L., Rowland, S.M., Rodgers, R.P., 2018a. Advances in asphaltene petroleomics. part 2: selective separation method that reveals fractions enriched in island and archipelago structural motifs by mass spectrometry. Energy Fuel. 32, 314–328. https://doi.org/10.1021/acs.energyfuels.7b03281.
Chacon-Patino, M.L., Rowland, S.M., Rodgers, R.P., 2018b. Advances in asphaltene petroleomics. Part 3. Dominance of island or archipelago structural motif is sample dependent. Energy Fuel. 32, 9106–9120. https://doi.org/10.1021/acs.energyfuels.8b01765.
Cheshkova, T.V., Kovalenko, E.Y., Sergun, V.P., et al., 2019a. Oil resins and asphaltenes of different chemical nature. Chem. Sustain. Dev. 1, 78–85. https://doi.org/10.15372/CSD20190113.
Cheshkova, T.V., Sergun, V.P., Kovalenko, E.Y., et al., 2019b. Resins and asphaltenes of light and heavy oils: composition and structure. Energy Fuel. 33, 7971–7982. https://doi.org/10.1021/acs.energyfuels.9b00285.
Dhand, V., Yadav, M., Kim, S.H., et al., 2021. A comprehensive review on the prospects of multi-functional carbon nano onions as an effective, high-performance energy storage material. Carbon 175, 534–575. https://doi.org/10.1016/j.carbon.2020.12.083.
Di Primio, R., Horsfield, B., Guzman-Vega, M.A., 2000. Determining the temperature of petroleum formation from the kinetic properties of petroleum asphaltenes. Nature 406, 173–176. https://doi.org/10.1038/35018046.
Dolomatov, M.Y., Shutkova, S.A., Bakhtizin, R.Z., et al., 2020. Structure of asphaltene molecules and nanoclusters based on them. Petrol. Chem. 60, 16–21. https://doi.org/10.1134/S0965544120010077.
Douda, J., Llanos, M.E., Alvarez, R., et al., 2004. Pyrolysis applied to the study of a Maya asphaltene. J. Anal. Appl. Pyrolysis 5, 24412–24421. https://doi.org/10.1021/acsomega.0c02792.
Fan, T.G., Wang, J.X., Buckley, J.S., 2002. Evaluating crude oils by SARA analysis. In: Proc. SPE/DOE Improved Oil Recovery Symposium. Tulsa, Oklahoma. https://doi.org/10.2118/75228-MS.
Galimova, G.A., Yusupova, T.N., Ibragimova, D.A., 2015. Composition, properties, structure and fractions of asphaltenes of the disperse petroleum systems. Vestnik KGTU 20, 60–64 (in Russian).
Ganeeva, Y.M., Yusupova, T.N., Romanov, G.V., 2011. Asphaltene nanoaggregates: structure, phase transformations, influence on properties of oil systems. Russ. Chem. Rev. 80, 1034–1050. https://doi.org/10.1070/RC2011v080n10ABEH004174.
Gerasimova, N.N., Cheshkova, T.V., Kovalenko, E.Y., et al., 2022. Composition of resin-asphaltene and oil components of heavy oils. Bulletin of the Tomsk Polytechnic University 333 (9), 128–136. https://doi.org/10.18799/24131830/2022/9/3672.
Ghabri, K., Benyounes, K., Khodja, M., 2017. Removal and prevention of asphaltene deposition during oil production: a literature review. J. Petrol. Sci. Eng. 158, 351–360. https://doi.org/10.1016/j.petrol.2017.08.062.
Glebovskaya, E.A., 1971. Use of Infrared Spectrometry in Petroleum Geochemistry. Nedra, Leningrad (in Russian).
Golovko, A.K., Gorbunova, L.V., Kam'yanov, V.F., 2010. The regularities in the structural group composition of high-molecular heteroatomic petroleum components. Russ. Geol. Geophys. 51 (3), 286–295. https://doi.org/10.1016/j.rgg.2010.02.005.
Golovko, A.K., Kam'yanov, V.F., Ogorodnikov, V.D., 2012. High-molecular heteroatomic components of crude oils of the Timan-Pechora petroliferous basin. Russ. Geol. Geophys. 53, 1374–1381. https://doi.org/10.1016/j.rgg.2010.02.005.
Golovko, A.K., Grinko, A.A., 2018. Structural transformations of petroleum resins and their fractions by thermolysis. Petrol. Chem. 58, 599–606. https://doi.org/10.1134/S0965544118080078.
Gomez, E., Rani, D.A., Cheeseman, C.R., et al., 2009. Thermal plasma technology for the treatment of wastes: a critical review. J. Hazard Mater. 161, 614–626. https://doi.org/10.1016/j.jhazmat.2008.04.017.
Gordadze, G., 2015. Hydrocarbons in petroleum geochemistry. In: Theory and Practice. Publishing Center of Russian State University of Oil and Gas, p. 559 (in Russian).
Gordadze, G., Kerimov, V., Giruts, M., et al., 2018. Genesis of the asphaltite of the Ivanovskoe field in the Orenburg region, Russia. Fuel 216, 835–842. https://doi.org/10.1016/j.fuel.2017.11.146.
Grinko, A.A., Golovko, A.K., 2011. Fractionation of resins and asphaltenes and investigation of their composition and structure using heavy oil from the USA field as an example. Petrol. Chem. 51, 192–202. https://doi.org/10.1134/S0965544111030066.
Grinko, A.A., Golovko, A.K., 2014. Thermolysis of petroleum asphaltenes and their fractions. Petrol. Chem. 54, 42–47. https://doi.org/10.1134/S0965544113040051.
Guo, K., Li, H., Yu, Z., 2016. In-situ heavy and extra-heavy oil recovery: a review. Fuel 185, 886–902. https://doi.org/10.1016/j.fuel.2016.08.047.
Han, Z., Kong, S., Cheng, G., et al., 2019. Preparation of efficient carbon-based adsorption material using asphaltenes from asphalt rocks. Ind. Eng. Chem. Res. 58 (32), 14785–14794. https://doi.org/10.1021/acs.iecr.9b02143.
He, C.N., Zhao, N.Q., Shi, C.S., et al., 2009. Effect of annealing on the structure of carbon onions and the annealed carbon coated Ni nanoparticles fabricated by chemical vapor deposition. J. Alloys Compd. 472. https://doi.org/10.1016/j.jallcom.2008.04.051, 2009.
Hontoria-Lucas, C., López-Peinado, A.J., López-González, J.D., et al., 1995. Study of oxygen-containing groups in a series of graphite oxides: physical and chemical characterization. Carbon 33, 1585–1592. https://doi.org/10.1016/0008-6223(95)00120-3.
Ivanova, L.V., Safieva, R.Z., Koshelev, V.N., 2008. IR spectrometry in the analysis of oil and petroleum products. Bull. Bashkir Univers. 13, 869–874 (in Russian).
Jung, H., Bielawski, K., 2019. Asphaltene oxide promotes a broad range of synthetic transformations. Commun. Chem. 2. https://doi.org/10.1038/s42004-019-0214-4.
Kamkar, M., Natale, G., 2021. A review on novel applications of asphaltenes: a valuable waste. Fuel 285, 119272. https://doi.org/10.1016/j.fuel.2020.119272.
Kananpanah, S., Kheirkhah, R., Bayat, M., et al., 2017. Comparison of asphaltene structure and morphology under different deasphaltene methods. Petrol. Sci. Technol. 35, 457–464. https://doi.org/10.1080/10916466.2016.1258416.
Katrick, B., Srivastava, S.K., Srivastava, I., 2013. Green synthesis of graphene. J. Nanosci. Nanotechnol. 13, 4320–4324. https://doi.org/10.1166/jnn.2013.7461.
Kayukova, G.P., Petrov, S.M., Uspensky, B.V., 2015. Properties of heavy oils and bitumens from the Permian deposits of Tatarstan in natural and technogenic processes. GEOS 1–342.
Kopytov, M.A., Golovko, A.K., 2017. Changes of structural group characteristics of heavy oils during their primary processing. Petrol. Chem. 57, 39–47. https://doi.org/10.1134/S0965544116090139.
Krayushkin, V.A., Guseva, E.E., Morozova, R.M., 2008. Geochemistry of porphyrins and the genesis of oil. Geol. 4, 26–38 (in Russian).
Letenko, D.G., Nikitin, V.A., Charykov, N.A., 2010. Synthesis of carbon nanostructures from waste products of chemical industry. Vestnik Grazhd. Inzhener. 1, 108–118 (in Russian).
Leyva, C., Ancheyta, J., Berrueco, C., et al., 2013. Chemical characterization of asphaltenes from various crude oils. Fuel Process. Technol. 106, 734–738. https://doi.org/10.1016/j.fuproc.2012.10.009.
Meshurova, T.A., Khodyashev, M.B., 2018. On the issue of reservoir and bottom water. Ekolog. Urbaniz. Territ. 4, 68–73 (in Russian).
Mohammadi, M.R., Ansari, S., Bahmaninia, H., et al., 2021. Experimental measurement and equilibrium modeling of adsorption of asphaltenes from various origins onto the magnetite surface under static and dynamic conditions. ACS Omega 6 (37), 24256–24268. https://doi.org/10.1021/acsomega.1c04224.
Montanari, L., Bonoldi, L., Alessi, A., et al., 2017. Molecular evolution of asphaltene from petroleum residues after different severity hydroconversion by EST process. Energy Fuel. 3, 3729–3737. https://doi.org/10.1021/acs.energyfuels.6b03332.
Mullins, O.C., Sheu, E.Y., Hammami, A., et al., 2007. Asphaltenes, Heavy Oils, and Petroleomics. Springer, New York, NY. https://doi.org/10.1007/0-387-68903-6.
Mullins, O.C., 2010. The modified yen model. Energy Fuel. 24 (4), 2179–2207. https://doi.org/10.1021/ef900975e.
Pak, A.Y., Bolatova, Z., Nikitin, D.S., et al., 2022a. Glass waste derived silicon carbide synthesis via direct current atmospheric arc plasma. Waste Manag. 144, 263–271. https://doi.org/10.1016/j.wasman.2022.04.002.
Pak, A.Y., Larionov, K.B., Kolobova, E.N., et al., 2022b. A novel approach of waste tires rubber utilization via ambient air direct current arc discharge plasma. Fuel Process. Technol. 227, 107–111. https://doi.org/10.1016/j.fuproc.2021.107111.
Petrova, Yu.Yu., Frantsina, E.V., Grinko, A.A., et al., 2022. Investigation of the process and products of plasma treatment of asphaltenes. Mater. Today Commun. https://doi.org/10.1016/j.mtcomm.2022.104669.
Poveda, J.C., Molina, D., Martinez, H., et al., 2014. Molecular changes in asphaltenes within H_2 plasma. Energy Fuel. 28, 735–744. https://doi.org/10.1021/ef401773t.

Raznoushkin, A.E., Khaibullin, A.A., Zhirnov, B.S., et al., 2015. On the possibility of using the polymeric-pitch compositions as the raw material for obtaining the carbon fibers. Neftepererabotka i neftechimiya 4, 27–33 (in Russian).
Saad, S., Zeraati, A.S., Roy, S., et al., 2022. Transformation of petroleum asphaltenes to carbon fibers. Carbon 190, 92–103. https://doi.org/10.1016/j.carbon.2022.01.011.
Schuler, B., Meyer, G., Pena, D., et al., 2015. Unraveling the molecular structures of asphaltenes by atomic force microscopy. J. Am. Chem. Soc. 137 (31), 9870–9876. https://doi.org/10.1021/jacs.5b04056.
Schuler, B., Fatayer, S., Meyer, G., et al., 2017. Heavy oil based mixtures of different origins and treatments studied by AFM. Energy Fuel. 31 (7), 6856–6861. https://doi.org/10.1021/acs.energyfuels.7b00805.
Siddiqui, M.N., Redhwi, H.H., Younas, M., et al., 2018. Use of asphaltene filler to improve low-density polyethylene properties. Petrol. Sci. Technol. 36 (11), 756–764. https://doi.org/10.1080/10916466.2018.1445105.
Skibichkaya, N.A., Burkhanova, I.O., Bolshakov, M.N., et al., 2016. Metal content in high-molecular-weight components of early oil (Case study – Orenburg Oil-Gas-Condensate Field). Proc. of Gubkin University 2, 23–34. https://doi.org/10.29222/ipng.2078-5712.2018-22.art35.
Socrates, G., 2004. Infrared and Raman Characteristic Group Frequencies: Tables and Charts, third ed. Wiley, Chichester.
Song, X., Liu, Y., Zhu, J., 2007. Synthesis of polyhedral graphite in a forced flow arc discharge. Mater. Lett. 61, 4781–4783. https://doi.org/10.1016/j.matlet.2007.03.032.
Strausz, O.P., Safarik, I., Lown, E.M., et al., 2008. A Critique of asphaltene fluorescence decay and depolarization-based claims about molecular weight and molecular architecture. Energy Fuel. 22 (2), 1156–1166. https://doi.org/10.1021/ef700320p.
Su, Y., Wei, H., Li, T., et al., 2014. Low-cost synthesis of single-walled carbon nanotubes by low-pressure air arc discharge. Mater. Res. Bull. 50, 23–25. https://doi.org/10.1016/S0379-6779(01)00563-X.
Temizel, C., Energy, A., Canbaz, C.H., et al., 2018. A comprehensive review heavy oil reservoirs, latest techniques discoveries, technologies and applications in the oil and gas industry. SPE-193646-MS. SPE International Heavy Oil Conference and Exhibition held in Kuwait City, Kuwait, 10–12 December. https://doi.org/10.2118/193646-MS.
Tikhomirov, S., Kimstach, T., 2011. Raman spectroscopy – a promising method for investigating carbon nanomaterials. Analítika 1, 28–32 (in Russian).
Ţucureanu, V., Matei, A., Marius, A., 2016. FTIR Spectroscopy for carbon family study. Crit. Rev. Anal. Chem. 46, 502–520. https://doi.org/10.1080/10408347.2016.1157013.
Usta, M., Ozbek, I., Bindal, C., et al., 2006. A comparative study of borided pure niobium, tungsten and chromium. Vacuum 80, 1321–1325. https://doi.org/10.1016/j.vacuum.2006.01.036.
Villa, M., Calixto-Rodriguez, M., Martinez, H., et al., 2010. Asphaltene surface erosion in air plasma. Plasma Sci. Technol. 12 (1), 81–86. https://doi.org/10.1088/1009-0630/12/1/17.
Wu, X., Ma, B., Xu, Y., et al., 2019. Preparation of three-layer graphene sheets from asphaltenes using a montmorillonite template. Nanomaterials, 2094723. https://doi.org/10.1155/2019/2094723.
Xu, C., Ning, C., Zhu, X., et al., 2013. Synthesis of graphene from asphaltene molecules adsorbed on vermiculite layers. Carbon 62, 213–221. https://doi.org/10.1016/j.carbon.2013.05.059.
Zhai, C., Kong, X., Hu, K., et al., 2020. Unexpected hydrogenation process in the formation of hydrogenated carbon nano-onions. Chem. Phys. Lett. 738, 136866. https://doi.org/10.1016/j.cplett.2019.136866.
Zhao, J., Su, Y., Yang, Z., et al., 2013. Arc synthesis of double-walled carbon nanotubes in low pressure air and their superior field emission properties. Carbon 58, 92–98. https://doi.org/10.1016/j.carbon.2013.02.036.
Zojaji, I., Esfandiarian, A., Taheri-Shakibd, J., 2021. Toward molecular characterization of asphaltene from different origins under different conditions by means of FT-IR spectroscopy. Adv. Colloid Interface Sci. 289, 102314. https://doi.org/10.1016/j.cis.2020.102314.